2021 43rd Annual International Conference of the
IEEE Engineering in Medicine & Biology Society (EMBC)
Oct 31 - Nov 4, 2021. Virtual Conference

Automatic Segmentation to Cluster Patterns of Breathing in Sleep Apnea

Villads Hulgaard Joergensen[1,2,3,4], Umaer Hanif[2,3,4], *Member, IEEE*, Poul Jennum[4], Emmanuel Mignot[3], Asbjoern W. Helge[2,3,4], and Helge B. D. Sorensen[2], *Senior Member, IEEE*

***Abstract*— Annotation of polysomnography (PSG) recordings for diagnosis of obstructive sleep apnea (OSA) is a standard procedure but an expensive and time-consuming process for clinicians. To aid clinicians in this process we present a data driven unsupervised hierarchical clustering approach for detection and visual presentation of breathing patterns in PSG recordings. The aim was to develop a model independent of manual annotations to detect and visualize respiratory events related to OSA. 10 recordings from the Sleep Heart Health Study database were used, and the proposed algorithm was evaluated based on the manually annotated events for each recording. The algorithm reached an F1-score of 0.58 across the 10 recordings when detecting the presence of an event vs. no event and a 100% correct diagnosis prediction of OSA when predicting if apnea-hypopnea index (AHI) $\geq$ 15, which is a clinically meaningful cut-off. The F1-score may be due to imprecise placement of events, difficulty distinguishing between hypopneas and stable breathing, and variations in scoring. In conclusion the performance can be improved despite the strong agreement in diagnostics. The method is a proof of concept that a clustering method can detect and visualize breathing patterns related to OSA while maintaining a correct diagnosis.**

I. INTRODUCTION

Obstructive sleep apnea (OSA) is a disorder with intermittent complete or partial obstruction of the upper airway during sleep. In most cases the obstruction is caused by the weight of fatty tissue around the neck, but may also be caused by individual anatomical features such as a narrow upper airway, mobility of the tongue or a protracted jaw. It is estimated that $\geq$14% of men and $\geq$5% of women worldwide suffer from OSA [1]. OSA patients have increased risk of stroke, heart attack and being in automobile accidents due to daytime drowsiness and fatigue. The gold standard for diagnosis of OSA is the apnea-hypopnea index (AHI) which is derived from annotations made by sleep technicians. The annotations are made on data from a sleep study in which a person's sleep is recorded on a polysomnogram (PSG) [1].

The gold standard may be inadequate for scoring different types of events i.e. apneas and hypopneas, but it is a good overall indication of whether an event occurred or not. Rosenberg et al. [2] found that the inter-scorer agreement of event vs. no event was 84.4%, but scoring specific types of events i.e. obstructive apneas and hypopneas the agreement scores fell to 77.1% and 65.4%, respectively [2].

We propose an unsupervised, data driven approach to aid technicians using an automated visual tool to increase consistent scoring. Few studies have used unsupervised learning on OSA. In [3], the primary goal was to predict mortality based on clusters from annotated OSA phenotypes and demographic values. The size of the dataset was therefore much larger than the data set used in this paper. In [4] unsupervised learning was used to classify sleep apnea vs. normal breathing using only ECG. The two papers used generalized characteristics of OSA from annotations, but did not investigate breathing patterns for each recording. The novelty of our paper is that the algorithm is independent of annotations and that the analysis is patient specific.

II. DATA DESCRIPTION

10 recordings from the Sleep Heart Health Study (SHHS) [5], [6] were used in this study. The goal of the SHHS was to test whether sleep disordered breathing is associated with an increased risk of cardiovascular diseases and mortality using follow-up studies on patients after their initial visit. The database consists of 6441 PSG recordings from men and women aged $\geq$ 40. The specific recordings used in this study were 200007, 200009, 200032, 200035, 200038, 200050, 200059, 200070, 200074, and 200078. These recordings were chosen due to the high number of annotated respiratory events. The signals used from each recording were nasal airflow, oxygen saturation, and heart rate. From the annotations the scored wake segments were used in the algorithm, and the annotations of obstructive apneas and hypopneas were used in the validation process.

III. PRE-PROCESSING

A. Nasal Airflow

The airflow signal (S_{air}) was standardized in individual segments of wake and segments of sleep to reduce the influence of recording anomalies and amplitude variations related to the recording equipment and placement thereof. The standardization was done on each segment individually by subtracting the segment mean and dividing by the segment standard deviation as shown in Eq. 1.

$$S_{air}(x) = \frac{S_{air}(x) - \frac{\sum_{x_i}^{x_{i+1}} S_{air}(x)}{x_{i+1} - x_i}}{std(S_{air}(x))}. \quad (1)$$

Here x_i is the starting value of the i'th segment of S_{air}.

*This work was not supported by any organization

[1] Corresponding Author: villads.joergensen@gmail.com

[2] Department of Health Technology, The Technical University of Denmark, Kgs. Lyngby, Denmark

[3] Stanford Center for Sleep Sciences and Medicine, Stanford University, Palo Alto, CA, USA.

[4] Danish Center for Sleep Medicine, Department of Neurophysiology, Rigshospitalet, Glostrup, Denmark.

B. Heart Rate and Oxygen Saturation

The Savitzky Golay (SG) filter [7] works as a low-pass filter and was used to smooth out high frequency peaks in the signals. This is important when finding local maxima and minima of the signals. The advantage of the (SG) filter is that the filter coefficients are not equal as they are determined by the polynomial degree. In contrast, the moving average filter operates with fixed filter coefficients which is rigid in a setting where the signals vary a lot, such as physiological signals from a PSG. The SG filter is denoted ($SG_{u,i}$) where u is the number of samples used for polynomial estimations and i is the polynomial order. Both the heart rate (HR) and oxygen saturation (SaO_2) signals were smoothed due to their rough edges caused by the sampling rate of 1 Hz.

IV. METHODS

We wanted to automatically detect variations in breathing related to OSA. Thus, we developed an algorithm that utilizes changes in the envelope of S_{air} to segment the signal. The segments were then directly translated to HR and indirectly to SaO_2 via a delay algorithm. Features were extracted from each segment in all three signals and then utilized in an agglomerative hierarchical clustering yielding four clusters and a label for each of the segments. This label could then be used to compare segments to manually annotated events.

A. Envelope Extraction

The purpose of envelope extraction was to derive overall changes in breathing inspired by [8]. Cubic spline interpolation (CSI) was used to generate the upper and lower envelope of S_{air}. The CSI had starting and end-points ($CSI_{g,h}$), where g is the starting index (usually 0) and h is the new length of the interpolated signal. The envelopes were extracted by interpolating detected local maxima using $CSI_{0,Q}$, where Q is the length of S_{air}. Subsequently, the envelope was smoothed twice with a SG filter; first $SG_{301,2}$ and then $SG_{201,2}$. The upper envelope was extracted as described above, whereas the lower envelope was extracted by flipping S_{air}, i.e. changing the sign of the signal, then detecting local maxima and flipping it back again. The peaks were then used to generate the envelope.

B. Segmentation

The aim of segmentation was to obtain quasi-stationary segments of S_{air} and to use these in a clustering scheme to locate breathing patterns that are alike. The segmentation was done using a smoothed combination of the upper and lower envelope (Env_{comb}) obtained by adding the upper envelope and the absolute value of the lower envelope together. The segment boundaries were found by locating where Env_{comb} changes most by finding the maxima of the smoothed derivative of Env_{comb} ($DEnv_{comb}$) as shown in Eq. 2. The local maxima were set to be at least 8 samples apart. The start index value of the segment was defined as $a(x_s)$ and the stop index value was defined as $a(x_{s+1})$.

$$DEnv_{comb}(x) = SG_{301,2}(SG_{301,2}(|\frac{\delta Env_{comb}(x)}{\delta(x)}|)). \quad (2)$$

C. Oxygen saturation delay

SaO_2 was included as this signal is directly related to cessation of breathing. The changes in this signal were thus important to detect OSA. In order to include features from SaO_2, an algorithm was developed to accommodate for the non-linear delay of SaO_2 in relation to $S_{airflow}$. The algorithm calculates the piece-wise linear correlation between the change in SaO_2 and Env_{comb} using a moving window (w) with 50% overlap. The change in SaO_2 was defined as the derivative of SaO_2 and is given by Eq. 3.

$$DSaO_2(x) = CSI_{0,K}(SG_{21_2}(\frac{\delta SaO_2(x)}{\delta(x)})). \quad (3)$$

The window size, dependent on signal length, is given by

$$w = \begin{cases} 600, & \text{if } Q \equiv 600 = 0 \\ 300, & \text{if } Q \equiv 600 \neq 0 \textbf{ and } K \equiv 300 = 0 \\ 100, & otherwise \end{cases} \quad (4)$$

The linear correlation was found using discrete linear convolution ($CC(m,l)$), where m and l are signals being correlated. The indices (v) of each window was defined as $v_0 = w$, $v_j = v_{j-1} + \frac{w}{2}$, $j \in [1,2,3,...,\frac{Q}{w}-2,\frac{Q}{w}-1,J = \frac{Q}{w}]$, thus J is the total number of windows. The signals and their windows were defined as in Eqs. 5a and 5b and the delay of the j'th window $h(j)$ was calculated as in Eqs. 5c and 5d:

$$m = DSaO_2(q),\ q \in [v_j, v_{j-1}] \quad (5a)$$

$$l = Env_{comb}(q),\ q \in [v_j, v_{j-1}] \quad (5b)$$

$$d(j) = |argmax(CC(m,l)) - w| \quad (5c)$$

$$h(j) = \begin{cases} 150, & \text{if } j = 0 \\ \frac{d(j)+d(j-1)}{2}, & \text{if } v_j \equiv w = 0 \\ & \textbf{and } 80 \leq d(j) \leq 500 \\ \frac{150+d(j-1)}{2}, & otherwise \end{cases} \quad (5d)$$

All delays across the recording were interpolated ($CSI_{0,Q}$) and smoothed with a $SG_{2400,2}$ filter to a continuous variable delay (VD). The delay constant (DC), defined in Eq. 6, i.e. amount each index value $a(x_s)$ and $a(x_{s+1})$ was delayed was defined as the mean of the $VD(x)$ in segment $Seg_B(x_s)$.

$$DC(x_s) = \frac{\sum_{x=x_s}^{x_{s+1}} VD(x)}{x_{s+1} - x_s}. \quad (6)$$

D. Features

Five features were extracted and used in the agglomerative hierarchical clustering using Ward's Linkage [9]. The features were chosen due to their physiological relevance to OSA and through an extensive investigation of various other features less informative and with low variance. Some features were dependent on the change and the direction of change in the signal ($Sig(x)$) i.e. the sign of the derivative of the slope of the signal. The sign was calculated as in Eq. 7.

$$sign_{Sig(x)}(x_s) = \sum_{x=\alpha}^{\beta} \frac{\delta Sig(x)}{\delta(x)}, \quad x \in [\alpha,\beta]. \quad (7)$$

*1) **Saturation change (SatC)**:* The *SatC* feature was chosen since it is used by technicians when scoring events and because pauses in breathing are seen as drops in SaO_2.

$$\Delta SaO_2(x) = max(SaO_2(x)) - min(SaO_2(x)) \quad (8a)$$

$$SatC(x_s) = \begin{cases} \Delta SaO_2(x_s), & \text{if } sign_{sat(x_s)}(x_s) \geq 0 \\ -\Delta SaO_2(x_s), & \text{if } sign_{sat(x_s)}(x_s) < 0 \end{cases} \quad (8b)$$

$x \in [\alpha = O_2a(x_s), \beta = O_2b(x_s)]$.

*2) **Envelope change (EnvC)**:* The *EnvC* was chosen since it reflects changes in breathing pattern, such as cessation of breathing after a segment of normal breathing.

$$\Delta Env_{up}(x_s) = max(Env_{up}(x)) - min(Env_{up}(x)) \quad (9a)$$

$$EnvC(x_s) = \begin{cases} \Delta Env_{up}(k_s), & \text{if } sign_{Env_{up}(x)}(x_s) \geq 0 \\ -\Delta Env_{up}(k_s), & \text{if } sign_{Env_{up}(x)}(x_s) < 0 \end{cases} \quad (9b)$$

x $\in [a(k_s), b(k_s)]$.

*3) **Arc length (ArcL)**:* The *ArcL* of the envelope was chosen since a normal breathing segment has a flat envelope and OSA related breathing segments cause changes to the envelope which change the arc length of the envelope.

$$L_{arc}(x_s) = \int_{x_s}^{x_{s+1}} |\frac{\delta Env_{up}(x)}{\delta(x)}| \quad (10a)$$

$$L_{sign}(x_s) = \sum_{x=x_s}^{\frac{x_s+x_{s+1}}{2}} \frac{\delta Env_{up}(x)}{\delta(x)} \quad (10b)$$

$$ArcL(x_s) = \begin{cases} L_{arc}, & \text{if } L_{sign}(x_s) \geq 0 \\ -L_{arc}, & \text{if } L_{sign}(x_s) < 0 \end{cases} \quad (10c)$$

*4) **Heart Rate Change (HRC)**:* The *HRC* feature was chosen since the heart rate is relatively stable during normal breathing and changes a lot during OSA events.

$$\Delta HR(x_s) = max(HR(x)) - min(HR(x)) \quad (11a)$$

$$HRC(x_s) = \begin{cases} \Delta HR(x_s), & \text{if } sign_{HR(x)}(x_s) \geq 0 \\ -\Delta HR(x_s), & \text{if } sign_{HR(x)}(x_s) < 0 \end{cases} \quad (11b)$$

x $\in [a(x_s), b(x_s)]$.

*5) **Standard Deviation** (Air_{STD}):* :

The Air_{STD} feature was chosen because it provides information about general amplitude changes in each segment.

$$Air_{STD}(x) = STD(S_{Air}(x_s)), \quad x \in [a(x_s), b(x_s)]. \quad (12)$$

E. Agglomerative Hierarchical Clustering

The goal of clustering the segments in an unsupervised, data-driven manner was to find breathing patterns that were alike without human intervention. All features extracted from each segment were stored in an $M \times N$ matrix, M being the number of segments and N the number of features. Prior to clustering, all features were standardized. The agglomerative hierarchical clustering (AHC) was set to generate four clusters using Ward's Linkage. Ward's Linkage was chosen because it, through visual inspection, performed better at clustering physiological relevant segments than linkage measures such as single, complete and average linkage. The label vector generated by the clustering was used to visualize the clustering and to check for acceptable cluster separation. Cluster separation inspection was done using Principal Component Analysis (PCA) [10].

To get meaningful results each recording was subject to visual inspection as the most separated clusters in the PCA were deemed apnea or recovery breathing, while the clusters in the middle were either hypopnea or (relatively) normal breathing. In order to asses this the labels were used to color the segments of the recording to visually inspect each cluster. After the four clusters had been assigned either "apnea", "hypopnea", "normal" or "recovery", the segments with their corresponding labels were compared to the manually annotated events. The "normal" and "recovery" clusters were combined to the predicted "No Event"-class in the classification.

F. Cluster and Annotation Comparison

The clustering of each segment was compared to the annotations by finding the segments which were overlapped by the manually scored annotations. If an annotation was overlapping more than one segment, the segment with most overlap was automatically chosen.

G. Prediction of AHI

As an indicator of how well the clustering performed for diagnostic purposes, a prediction scheme was made. It counted all segments with a 25% amplitude drop in the upper envelope. The amplitude drop was calculated as the minimum value of the segment divided by the maximum value of the previous segment as shown in Eq. 13. If the ratio between the two values was 0.75 or less and $SatC(x_s)$ was negative the $SatC(x_s)$ value was also stored. When comparing the AHI of the recording all the annotations that were placed within segments also scored as "wake" were not counted. This was because no segments within "wake" periods were used in the clustering. The criteria of having an AHI ≥ 15 was used to determine if a person had sleep apnea. Thus, the actual AHI value was only regarded in relation to AHI $\geq 15 \rightarrow$ sleep apnea, or AHI $< 15 \rightarrow$ no sleep apnea.

$$drop = \frac{min(Env_{up}(x_s))}{max(Env_{up}(x_{s-1}))}. \quad (13)$$

H. Performance Metrics

The F1-score was the primary performance metric in this study along with the sensitivity and specificity. These metrics were derived using the true positive (TP) values, the true negative values (TN), the false positive values (FP) and the false negative values (FN).

V. RESULTS AND DISCUSSION

In Table I the accuracy, sensitivity, specificity and F1-score of the three-class problem is shown. The algorithm best predicts the *No Event*-class. While apneas have a high accuracy and specificity, the sensitivity and F1-score is low making the predictions unreliable. Hypopnea predictions are worse, which may be explained by an overlap of the two classes, where the phenotypes of apneas and hypopneas in some instances resemble each other. The apnea and hypopnea clusters are separated, but closely related which may explain the misclassification. This may also explain why the two-class prediction is better. The results of the two-class prediction is shown in table II. When combining apneas and hypopneas into the *Event*-class the accuracy is 64%, but the sensitivity increases to 74% and the F1-score is 0.58. The high sensitivity shows that the probability of predicting an event is high when there is an event. This is important when evaluating the reliability of the algorithm. This behavior was also shown by Rosenberg et al. [2] as the inter-scorer agreement of event vs. no event was higher than that of the specific class. The inter-scorer agreement of event vs. no event was 84.4% and the inter-scorer agreement on apneas and hypopneas were 77.1% and 65.4%, respectively. For apneas, 14.4% were scored as hypopneas, and for hypopneas, 16.4% were scored as no event and 14.8% scored as obstructive apneas which also suggests that a two-class classification is better [2].

The validation through comparison poses a paradoxical problem, as the proposed method of detecting breathing patterns tries to avoid and challenge manually annotated events because of the low agreement between technicians. But the best way to validate the results is through comparison to the gold standard which is the method of manually annotated events, and thus the best performance standard. Due to the paradoxical nature of comparing the clustering to manually annotated events and to evaluate if diagnosis would be the same, the AHI prediction scheme was made. The AHI scheme predicts the same diagnosis in all 10 recordings when using only the changes in amplitude of the nasal airflow signal. Note, that the previous rules, by which the SHHS database was scored, did not include either desaturations or arousals as a requirement for scoring hypopneas, but focused mainly on the amplitude changes of the nasal airflow signal [6]. This may explain why the AHI prediction is the same when using only the envelope. As shown in table III it may also explain why the prediction becomes gradually worse as the oxygen saturation becomes a requirement because the oxygen saturation makes the scoring requirement more strict, and thus less events are scored with a stricter requirement, resulting in a lower AHI. Another factor to explain the gradually lower prediction rate is the oxygen saturation time delay. It has previously been shown that prediction of apneas and hypopneas from the oxygen saturation alone is plausible [12]. Therefore, a slightly wrong delay may have a significant impact on the segment boundaries for the oxygen saturation and thus the actual change found by the algorithm possibly leading to discrepancies during clustering. Finding the correct time delay was a significant hurdle, and something that could be revisited in future work, perhaps drawing inspiration from [14]. This is especially important when testing the algorithm on other cohorts scored by the current rules of the AASM since these require a 3% oxygen saturation drop or an arousal for scoring hypopneas [13]. It has to be noted that the results are from a data driven model with no training. The results are what the algorithm displays without human intervention. This is especially important when evaluating the results since the results reflect what the algorithm has found from the features. The features used in the study utilize different physiological signals to generate the clustering. When scoring sleep apnea, arousals play a role in detection of sleep apnea. Arousals have been used in the clustering indirectly through the change in heart rate as it is shown that heart rate and arousal intensity are highly correlated [11].

The features used in the study could be revisited in future work to increase performance. To make the method fully automatic, a wake stage detector should be implemented. The current method relies on the wake segments from the annotation sheet. This should be revisited in future studies. Data quality plays an important role when running the algorithm, and poor data quality is also subject to poor algorithm performance. For a data driven model to be completely reliable the data used must also be of good quality.

TABLE I
THREE-CLASS: APNEA VS. HYPOPNEA VS. NO EVENT

Apnea			
Accuracy	Sensitivity	Specificity	F1-score
0.85	0.51	0.89	0.42
Hypopnea			
Accuracy	Sensitivity	Specificity	F1-score
0.61	0.44	0.65	0.34
No event			
Accuracy	Sensitivity	Specificity	F1-score
0.64	0.59	0.74	0.69

TABLE II
TWO-CLASS: HYPOPNEA AND APNEA VS. NO EVENT

Hypopnea + Apnea			
Accuracy	Sensitivity	Specificity	F1-score
0.64	0.74	0.59	0.58

TABLE III
AHI PREDICTION

AHI $\geq$ 15

Recordings	E	0.5%	1%	2%	3%
10	10	9	7	4	2
Correct	100%	90%	70%	40%	20%

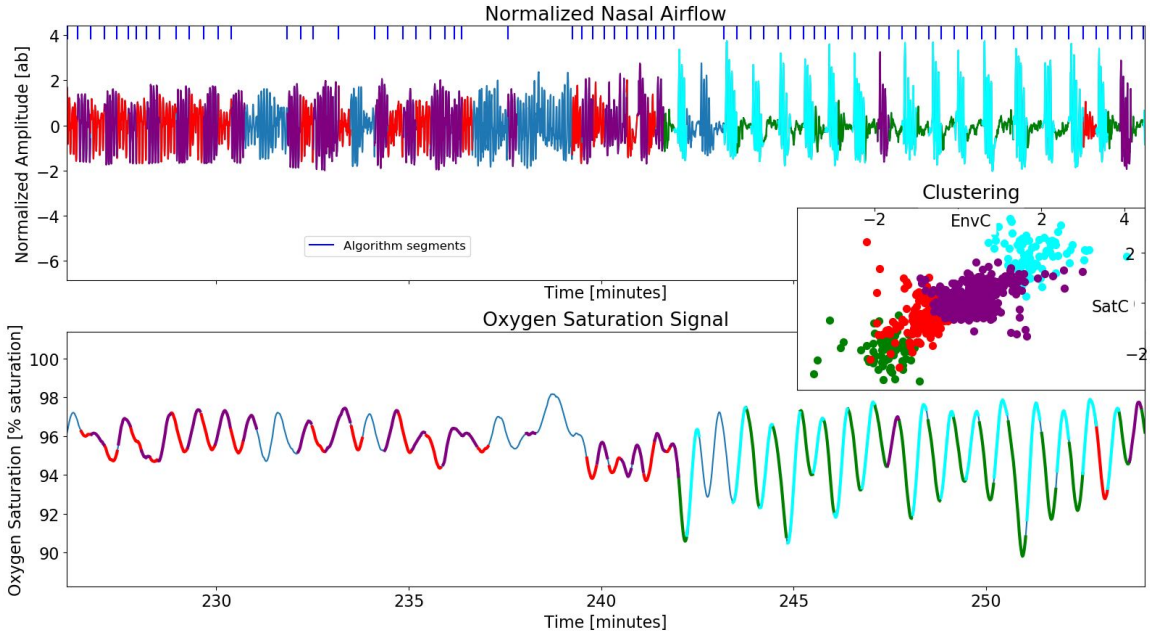

Fig. 1. **Top:** The nasal airflow signal with coloring according to which cluster each segment belongs to using the proposed hierarchical clustering. The ordinate axis is in arbitrary units due the preprocessing of the signal. The dark blue parts of the signal are annotated wake periods. The deep blue lines at the top are segment boundaries found by the segmentation algorithm. **Bottom:** The oxygen saturation signal. The blue parts of the signal are annotated wake periods. The signal segments are colored according to the corresponding segment in the above plot of the nasal airflow. Note the segments are slightly shifted due to the oxygen saturation delay. **Right:** The clustering plotted against two features (Envelope change (*EnvC*) and saturation change (*SatC*)).

Using another envelope-based method like [8] could perhaps increase performance with removal of artifact, but cannot make up for noise and poor data quality due to equipment that has shifted during the night. The recordings used in the study contains a high number of respiratory events. This was a deliberate decision because the clustering also performs best with high variance in the data. To generalize the findings from this study the algorithm should be tested on more recordings from different cohorts to verify the findings in this study.

VI. CONCLUSIONS

The goal of this paper was to develop an algorithm to assist technicians with consistent scoring. The performance of the algorithm was best when regarding event versus no event with an accuracy of 64%, sensitivity of 74%, specificity of 59% and an F1-score of 0.58. Accuracy of predicting AHI $\geq$ 15 was 100% when using only the envelope to score events, and falling linearly when a drop in oxygen saturation became a requirement. The algorithm can be improved, but serves as a proof of concept that a data driven model can be used to detect and visualize breathing patterns in PSG recordings to aid technicians with annotations, which in turn helps clinicians derive better diagnoses for sleep apnea patients.

ACKNOWLEDGMENT

We would like to thank the National Sleep Research Resource team for their efforts in collecting, organizing and making available the PSG data used in this study.

REFERENCES

[1] Kapur, Vishesh K., et al. “Clinical practice guideline for diagnostic testing for adult obstructive sleep apnea: An American academy of sleep medicine clinical practice guideline”, J Clin Sleep Med, vol. 13, no. 3, pp. 479–504, 2017.
[2] Rosenberg, Richard S. and Van Hout, Steven, “The American Academy of Sleep Medicine inter-scorer reliability program: Respiratory events”, J Clin Sleep Med, vol. 10, no. 4, 2014.
[3] Ma, Eun Yeol, et al. “Combined Unsupervised-Supervised Machine Learning for Phenotyping Complex Diseases with Its Application to Obstructive Sleep Apnea”, Scientific Reports, vol. 11, no. 4457, 2021.
[4] Feng, Kaicheng, et al. “A Sleep Apnea Detection Method Based on Unsupervised Feature Learning and Single-Lead Electrocardiogram”, IEEE Trans Instrum Meas, vol. 70, pp. 1-12, 2020.
[5] Zhang, Guo Qiang, et al. “The National Sleep Research Resource: Towards a sleep data commons”, J Am Med Inform Assn, vol. 25, no. 10, pp. 1351–1358, 2018.
[6] Quan, Stuart F., et al. “The Sleep Heart Health Study: Design, rationale, and methods”, Sleep, vol. 20, no. 12, pp. 1077–1085, 1997.
[7] Schafer, Ronald W., “What is a savitzky-golay filter?”, IEEE Signal Process Mag, vol. 28, no. 4, pp. 111-117, 2011.
[8] Ciolek, Marcin, et al. “Automated detection of sleep apnea and hypopnea events based on robust airflow envelope tracking in the presence of breathing artifacts”, IEEE J Biomed Health Inform, vol. 19, no. 2, pp. 418-429, 2014.
[9] Ward, Joe H., “Hierarchical Grouping to Optimize an Objective Function”, J Am Stat Assoc, vol. 58, no. 301, pp. 236-244, 1963.
[10] Runkler, Thomas A., “Data analytics: models and algorithms for intelligent data analysis”, Data Analytics, book, 2020.
[11] Azarbarzin, Ali, et al. “Relationship between arousal intensity and heart rate response to arousal”, Sleep, vol. 37, no. 4, pp. 645-653, 2014.
[12] Rolon, R. E., et al. “Automatic scoring of apnea and hypopnea events using blood oxygen saturation signals”, Biomed Signal Process Control, vol. 62, 2020.
[13] Berry, R. B., et al. “AASM Scoring Manual”, 2017 (version 2.4).
[14] Gutta, Sandeep and Cheng, Qi., “A Modeling of oxygen saturation and respiration for sleep apnea detection”, 50th Asilomar Conference on Signals, Systems and Computers, IEEE, 2016